Supplement of Atmos. Chem. Phys., 20, 6479–6493, 2020
https://doi.org/10.5194/acp-20-6479-2020-supplement

Atmospheric Chemistry and Physics
Open Access

Supplement of

The mechanisms and seasonal differences of the impact of aerosols on daytime surface urban heat island effect

Wenchao Han et al.

Correspondence to: Zhanqing Li (zli@atmos.umd.edu)

Contents of this file

Figures S1-S9

Tables S1-S3

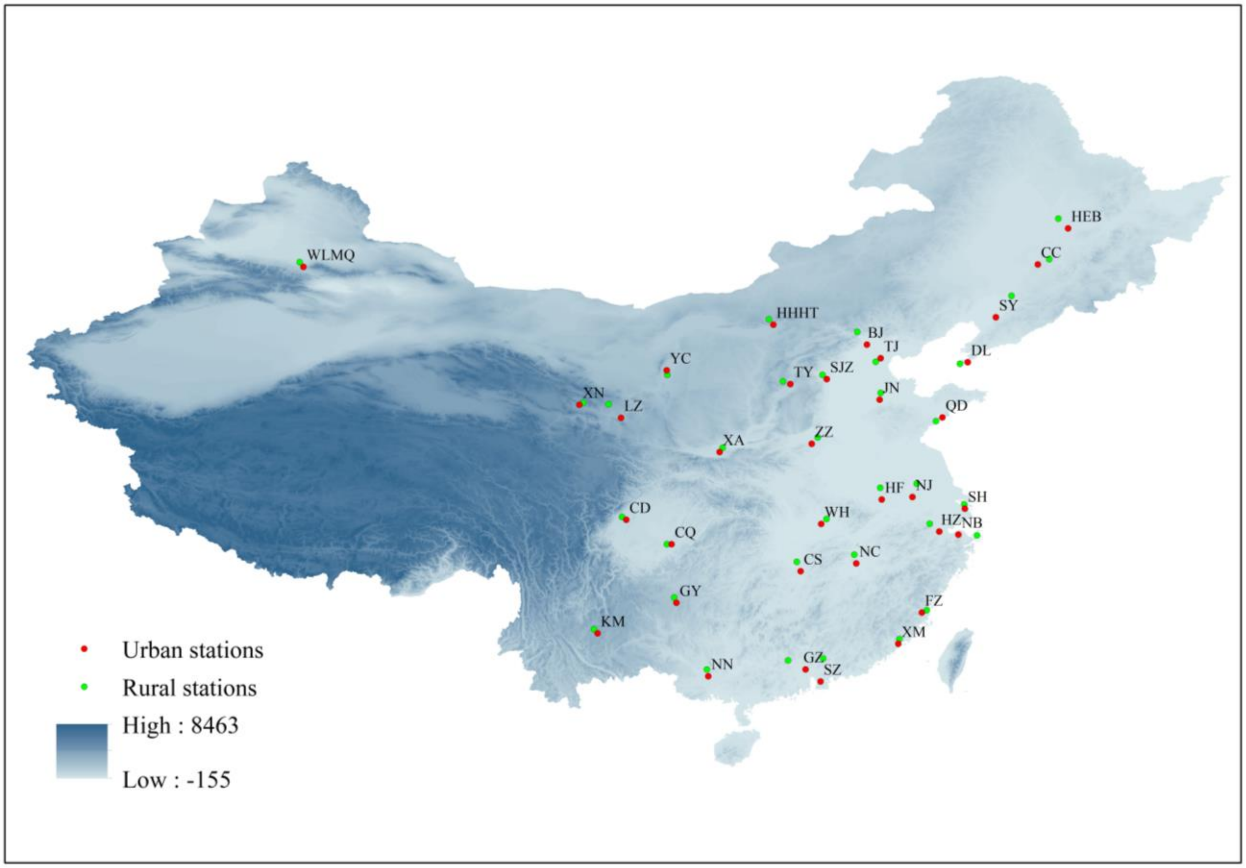

Figure S1. Spatial distribution of meteorological stations located in 35 cities.

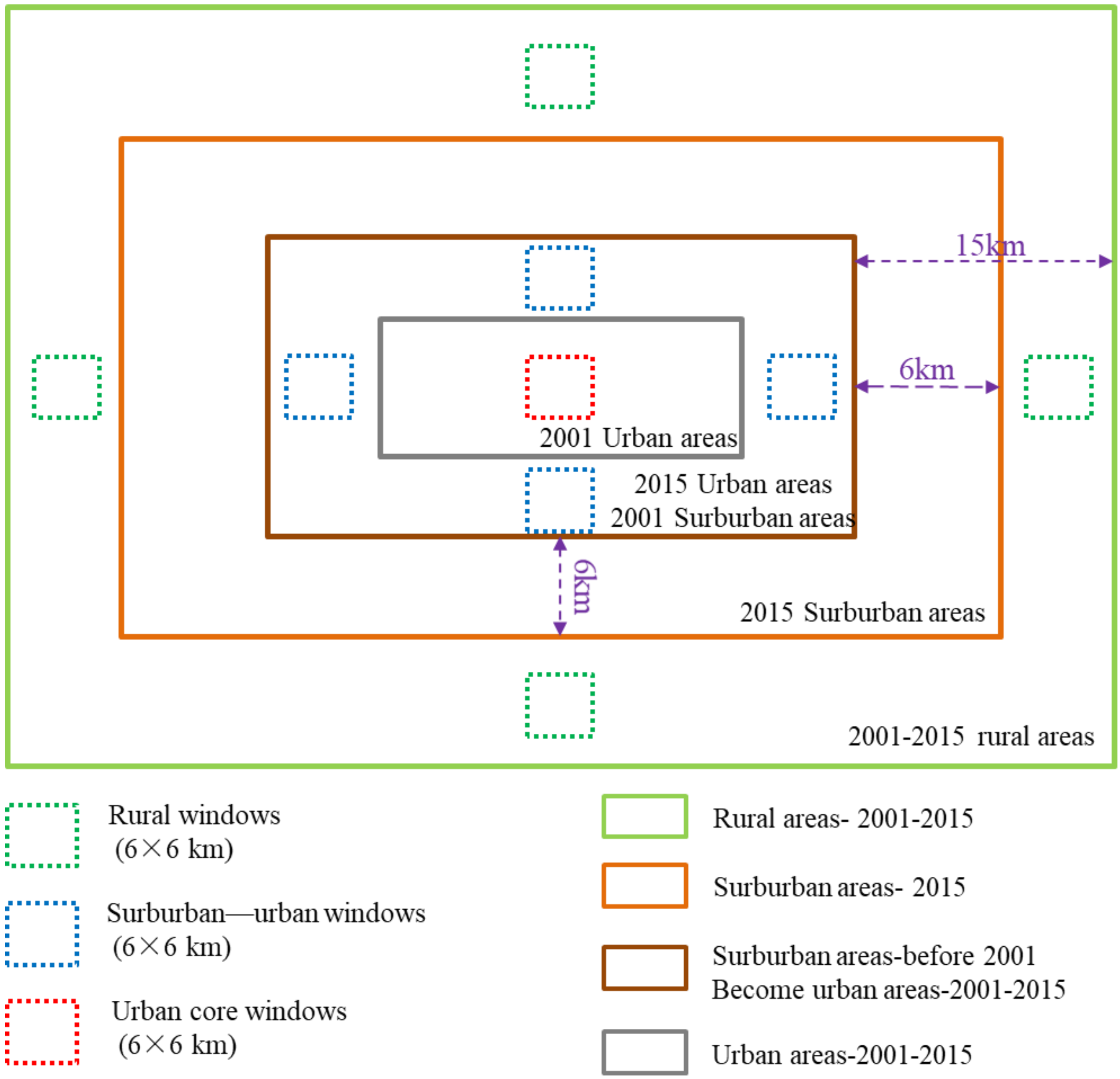

Figure S2. Schematic diagram showing the spatial distribution of the nine research windows for a given city.

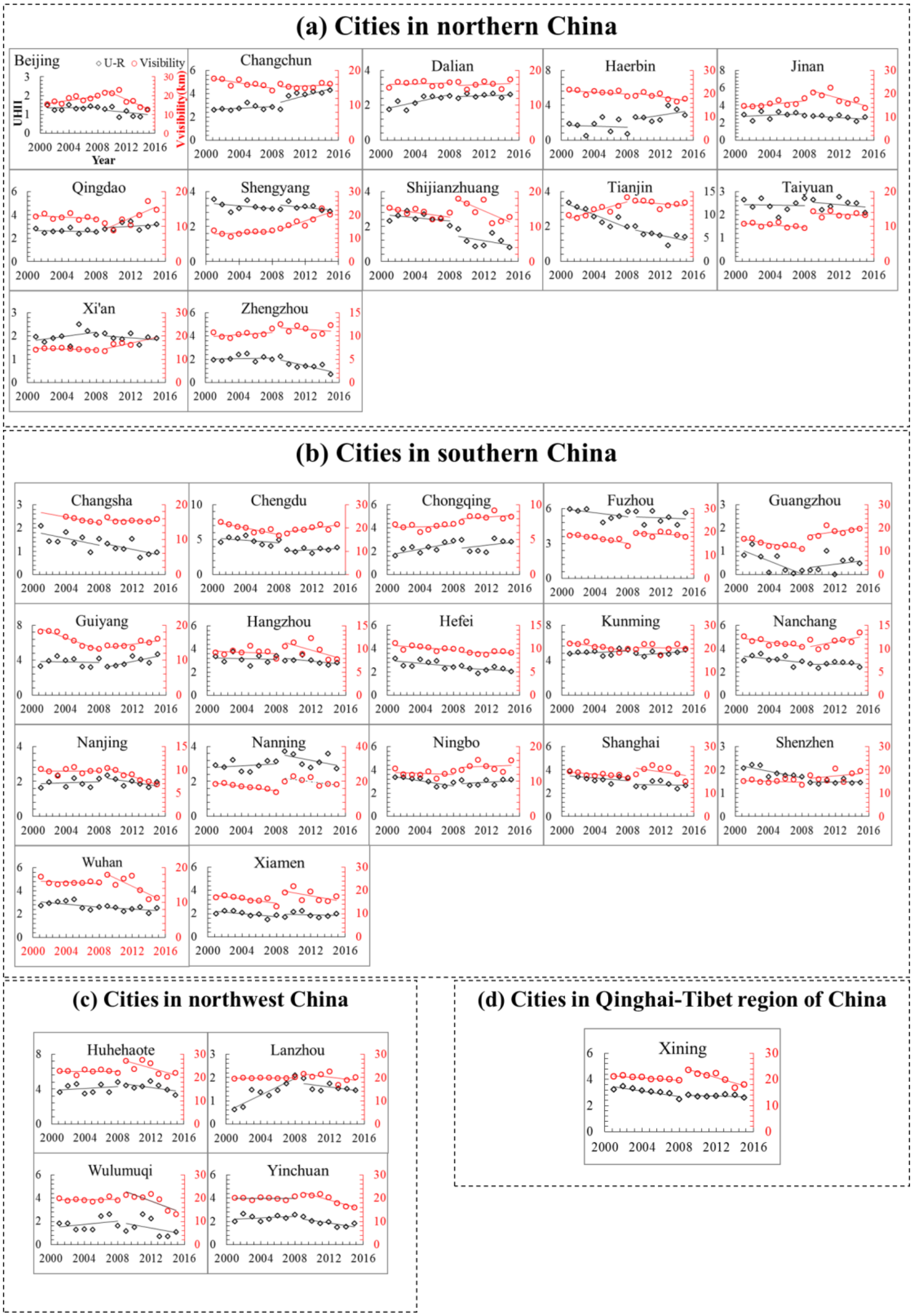

Figure S3. Clear-day UHII (black lines, unit: K) and visibility (red lines, unit: km) trends at the 35 cities divided by region: (a) northern China, (b) southern China, (c) northwest China, and (d) the Qinghai-Tibet region for the period 2001 to 2015.

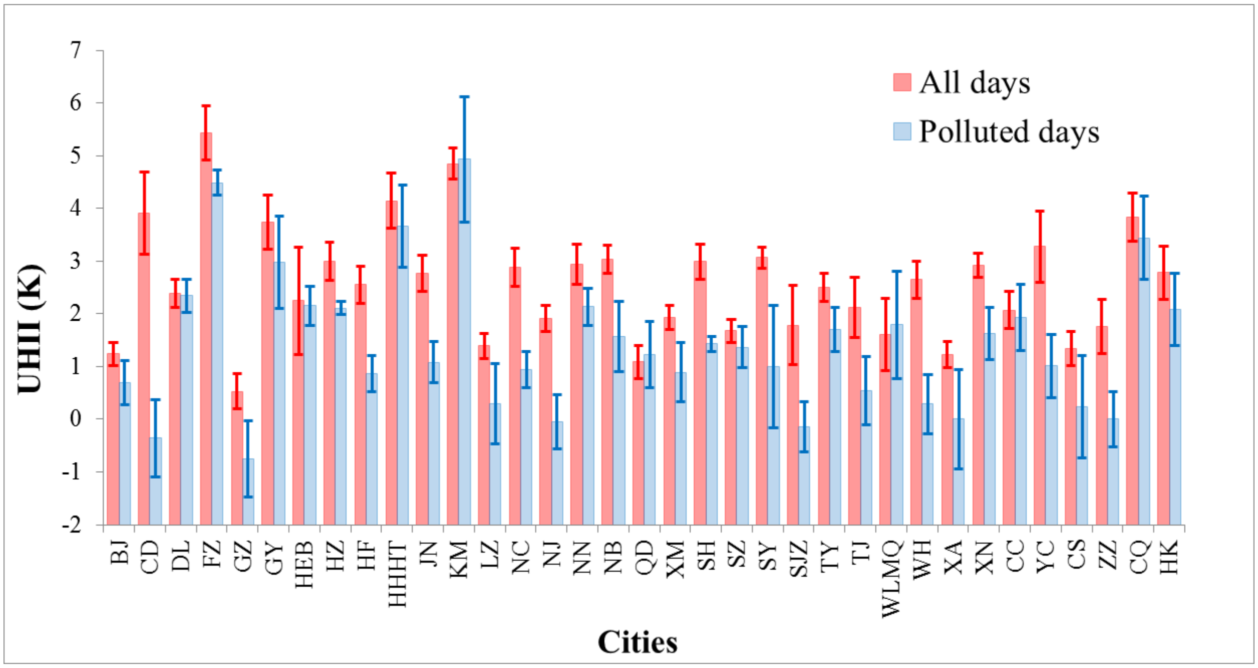

Figure S4. Mean UHII (unit: K) for each city under polluted conditions (blue bars) and for all days (red bars) on an annual scale.

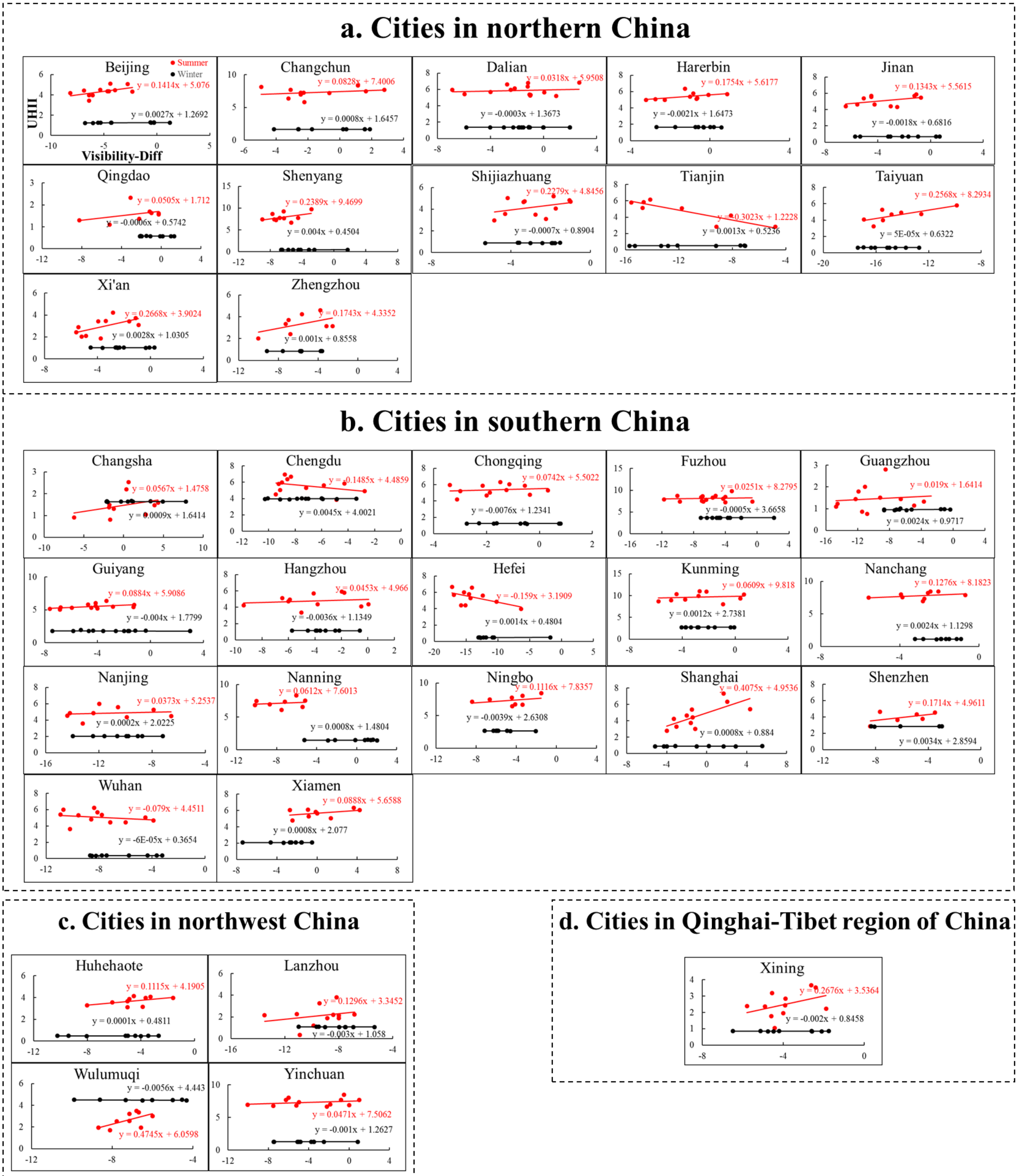
a. Cities in northern China
Beijing
Summer
Winter
UHII
Visibility-Diff
y = 0.1414x + 5.076
y = 0.0027x + 1.2692
Changchun
y = 0.0828x + 7.4006
y = 0.0008x + 1.6457
Dalian
y = 0.0318x + 5.9508
y = -0.0003x + 1.3673
Harerbin
y = 0.1754x + 5.6177
y = -0.0021x + 1.6473
Jinan
y = 0.1343x + 5.5615
y = -0.0018x + 0.6816
Qingdao
y = 0.0505x + 1.712
y = -0.0006x + 0.5742
Shenyang
y = 0.2389x + 9.4699
y = 0.004x + 0.4504
Shijiazhuang
y = 0.2279x + 4.8456
y = -0.0007x + 0.8904
Tianjin
y = -0.3023x + 1.2228
y = 0.0013x + 0.5236
Taiyuan
y = 0.2568x + 8.2934
y = 5E-05x + 0.6322
Xi'an
y = 0.2668x + 3.9024
y = 0.0028x + 1.0305
Zhengzhou
y = 0.1743x + 4.3352
y = 0.001x + 0.8558
b. Cities in southern China
Changsha
y = 0.0567x + 1.4758
y = 0.0009x + 1.6414
Chengdu
y = 0.1485x + 4.4859
y = 0.0045x + 4.0021
Chongqing
y = 0.0742x + 5.5022
y = -0.0076x + 1.2341
Fuzhou
y = 0.0251x + 8.2795
y = -0.0005x + 3.6658
Guangzhou
y = 0.019x + 1.6414
y = 0.0024x + 0.9717
Guiyang
y = 0.0884x + 5.9086
y = -0.004x + 1.7799
Hangzhou
y = 0.0453x + 4.966
y = -0.0036x + 1.1349
Hefei
y = -0.159x + 3.1909
y = 0.0014x + 0.4804
Kunming
y = 0.0609x + 9.818
y = 0.0012x + 2.7381
Nanchang
y = 0.1276x + 8.1823
y = 0.0024x + 1.1298
Nanjing
y = 0.0373x + 5.2537
y = 0.0002x + 2.0225
Nanning
y = 0.0612x + 7.6013
y = 0.0008x + 1.4804
Ningbo
y = 0.1116x + 7.8357
y = -0.0039x + 2.6308
Shanghai
y = 0.4075x + 4.9536
y = 0.0008x + 0.884
Shenzhen
y = 0.1714x + 4.9611
y = 0.0034x + 2.8594
Wuhan
y = -0.079x + 4.4511
y = -6E-05x + 0.3654
Xiamen
y = 0.0888x + 5.6588
y = 0.0008x + 2.077
c. Cities in northwest China
Huhehaote
y = 0.1115x + 4.1905
y = 0.0001x + 0.4811
Lanzhou
y = 0.1296x + 3.3452
y = -0.003x + 1.058
Wulumuqi
y = -0.0056x + 4.443
y = 0.4745x + 6.0598
Yinchuan
y = 0.0471x + 7.5062
y = -0.001x + 1.2627
d. Cities in Qinghai-Tibet region of China
Xining
y = 0.2676x + 3.5364
y = -0.002x + 0.8458

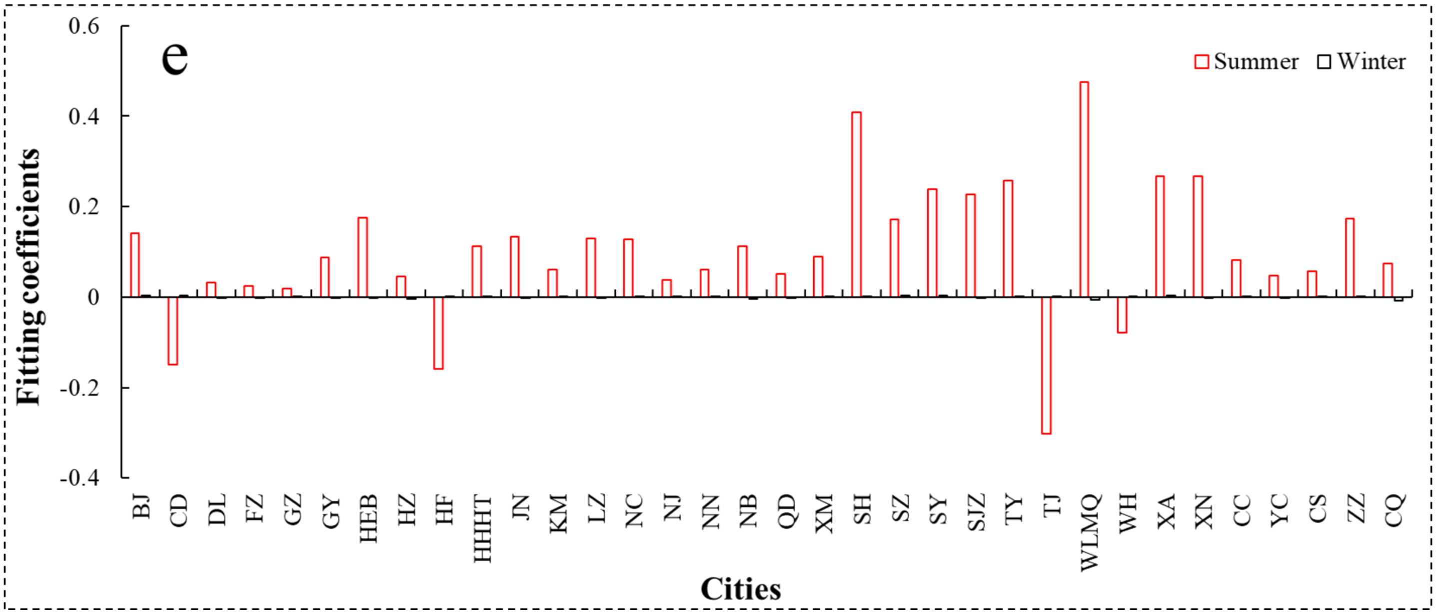

Figure S5. Relationship between UHII (unit: K) and visibility differences (unit: km) at the 35 cities divided by region in summer (red points and lines) and winter (black points and lines) when the RH is less than 85 %: (a) northern China, (b) southern China, (c) northwest China, and (d) the Qinghai-Tibet region. (e) Fitting coefficients of all cities for the period 2001 to 2015.

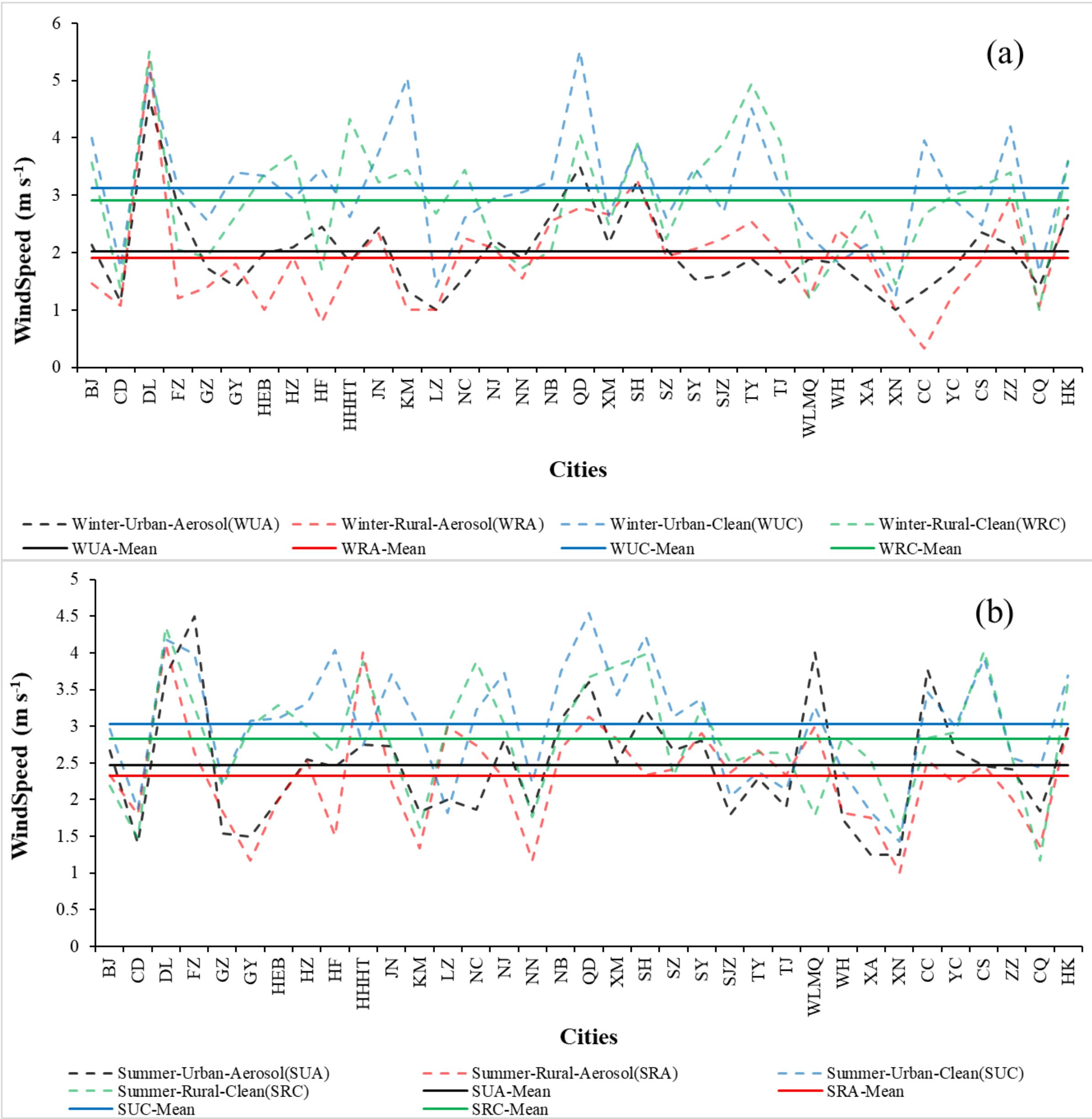

Figure S6. Comparison of wind speeds (unit: m s^{-1}) between urban and rural areas under heavy air pollution and clean conditions in (a) winter and (b) summer. City-specific values for each city: The black and red dashed curves show the urban and rural wind speeds, respectively, under polluted conditions. The blue and green dashed curves show the urban and rural wind speeds, respectively, under clean conditions. Considering all cites: The black and red horizontal lines show the mean urban and rural wind speeds, respectively, under polluted conditions. The blue and green horizontal lines show the mean urban and rural wind speeds, respectively, under clean conditions.

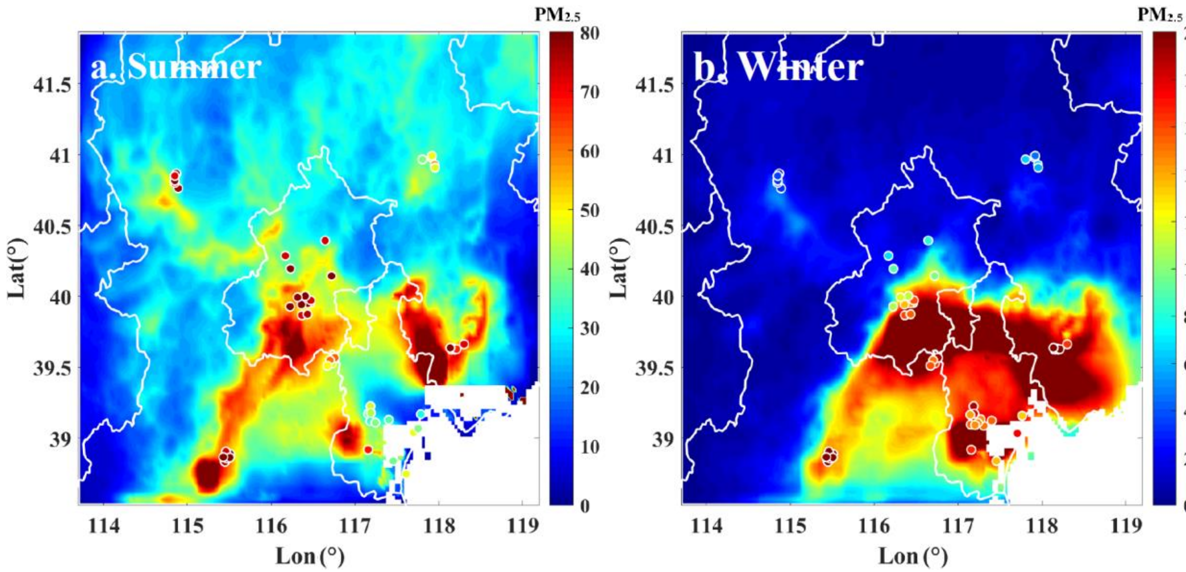

Figure S7. Comparisons of simulated distributions of $PM_{2.5}$ concentration (color map, unit: μg m^{-3}) and ground-measured $PM_{2.5}$ concentrations (colored dots, unit: μg m^{-3}) on typical days in (a) summer and (b) winter. Table S2 gives the time periods for the analysis.

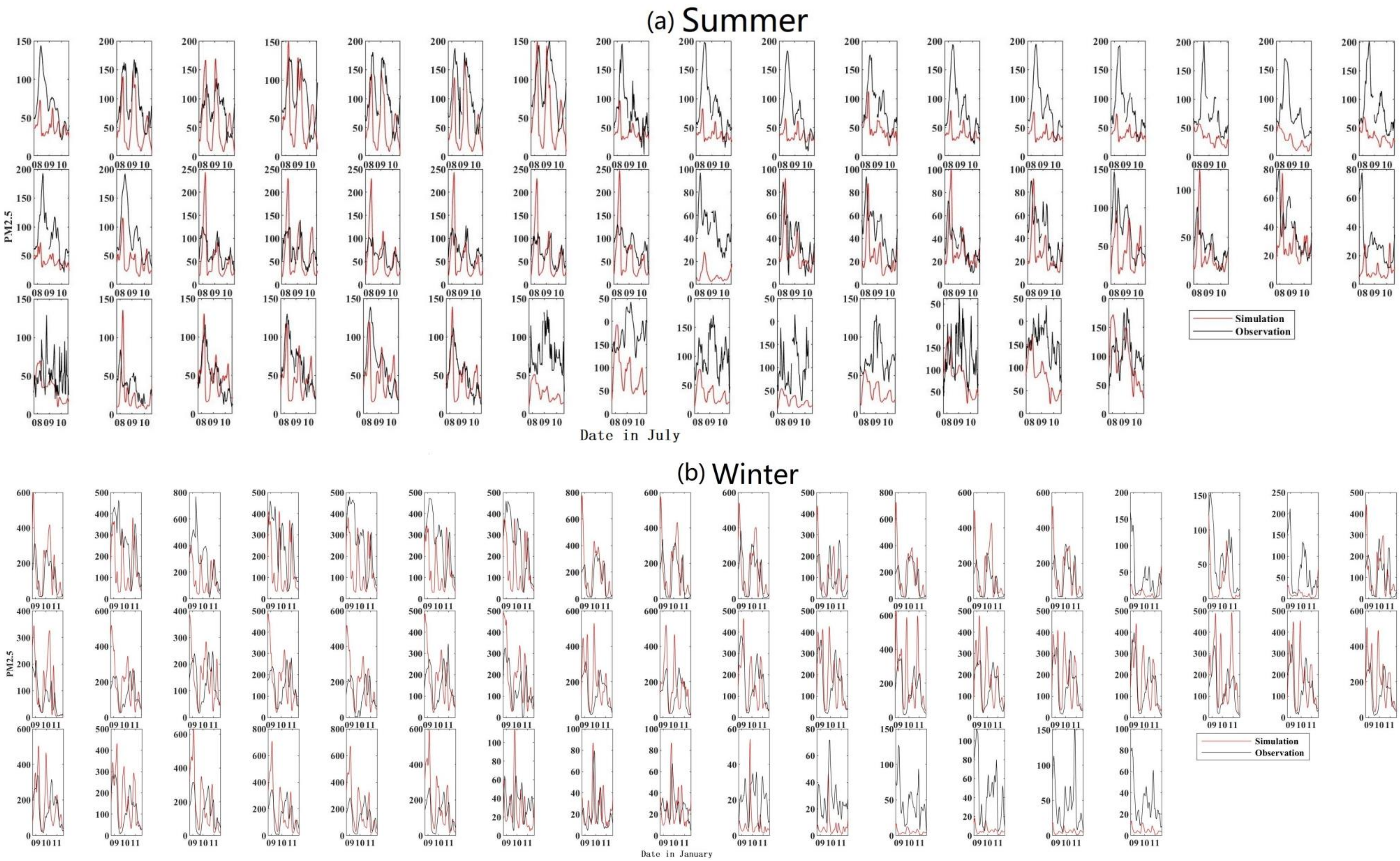

Figure S8. Simulated (red curves) and observed (black curves) temporal trends in $PM_{2.5}$ concentration (unit: ug m^{-3}) at each site in (a) summer (8 July to 10 July 2015) and (b) winter (7 January to 10 January 2015).

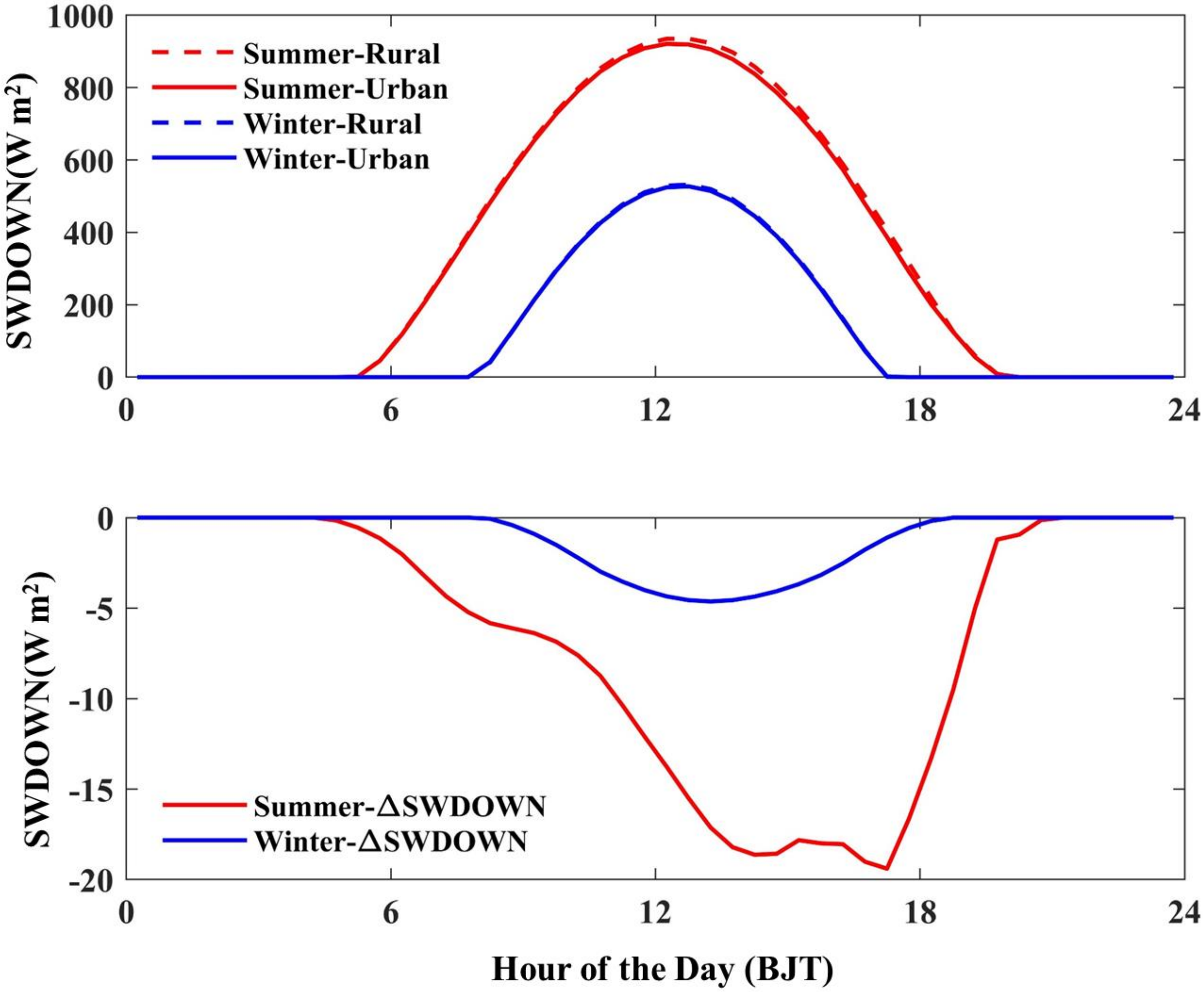

Figure S9. (a) Mean diurnal variations in downward shortwave radiation at the surface (SWDOWN) with the ARE (unit: W m^{-2}) during the course of typical days in summer (6 July to 10 July 2015) and winter (7 January to 10 January 2015). Solid and dashed lines represent urban and rural trends, respectively. (b) Diurnal variation in SWDOWN differences (unit: W m^{-2}). $\Delta SWDOWN$ is the SWDOWN difference between urban and rural areas. The blue and red curves represent winter and summer, respectively.

Table S1. Schemes of the simulations used in WRF-Chem3.9.1.

Type of scheme	Options
Microphysics scheme	Morrison et al. (Morrison et al., 2009)
Radiation scheme	RRTMG (Iacono et al., 2008)
surface-layer option	Monin-Obukhov scheme (Monin and Obukhov, 1954)
Land surface scheme	Noah LSM with single-layer UCM (Chen and Dudhia, 2001; Kusaka et al., 2001; Kusaka and Kimura, 2004)
PBL scheme	YSU (Hong et al., 2006)
Chemical mechanism	Carbon Bond Mechanism, version Z
Aerosol model	MOSAIC (8 bins) (Zaveri and Peters, 1999; Zaveri et al., 2008)

References

Chen, F. and Dudhia, J.: Coupling an advanced land surface–hydrology model with the Penn State–NCAR MM5 modeling system. Part I: Model implementation and sensitivity, Mon. Weather Rev., 129(4), 569–585, https://doi.org/10.1175/1520-0493(2001)129<0569:CAALSH>2.0.CO;2, 2001.

Hong, S. Y., Noh, Y., and Dudhia, J.: A new vertical diffusion package with an explicit treatment of entrainment processes, Mon. Weather Rev., 134(9), 2318–2341, https://doi.org/10.1175/MWR3199.1, 2006.

Iacono, M. J., Delamere, J. S., Mlawer, E. J., Shephard, M. W., Clough, S. A., and Collins, W. D.: Radiative forcing by long-lived greenhouse gases: calculations with the AER radiative transfer models, J. Geophys. Res. Atmos., 113(D13), https://doi.org/10.1029/2008JD009944, 2008.

Kusaka, H. and Kimura, F.: Coupling a single-layer urban canopy model with a simple atmospheric model: Impact on urban heat island simulation for an idealized case, J. Meteorol. Soc. Jpn. Ser. II, 82(1), 67–80, https://doi.org/10.2151/jmsj.82.67, 2004.

Kusaka, H., Kondo, H., Kikegawa, Y., and Kimura, F.: A simple single-layer urban canopy model for atmospheric models: comparison with multi-layer and slab models, Bound.-Lay. Meteorol., 101(3), 329–358, https://doi.org/10.1023/A:1019207923078, 2001.

Monin, A. S. and Obukhov, A. M.: Basic laws of turbulent mixing in the surface layer of the atmosphere, Contrib. Geophys. Inst. Acad. Sci. USSR, 151(163), e187.

Morrison, H., Thompson, G., and Tatarskii, V.: Impact of cloud microphysics on the development of trailing stratiform precipitation in a simulated squall line: comparison of one-and two-moment schemes, Mon. Weather Rev., 137(3), 991–1007, https://doi.org/10.1175/2008MWR2556.1, 2009.

Zaveri, R. A. and Peters, L. K.: A new lumped structure photochemical mechanism for large-scale applications, J. Geophys. Res. Atmos., 104(D23), 30,387–30,415, https://doi.org/10.1029/1999JD900876, 1999.

Zaveri, R. A., Easter, R. C., Fast, J. D., and Peters, L. K.: Model for simulating aerosol interactions and chemistry (MOSAIC), J. Geophys. Res. Atmos., 113(D13), https://doi.org/10.1029/2007JD008782, 2008.

Table S2. Time periods (yyyymmdd, where yyyy = year, mm = month, and dd = day) and the aerosol effect used for WRF-Chem experiments.

Experiments	Study period	Description
A1Summer	20150707–20150710	Switch on aerosol radiative effect
A0Summer	20150707–20150710	Switch off aerosol radiative effect
A1Winter	20150108–20150110	Switch on aerosol radiative effect
A0Winter	20150108–20150110	Switch off aerosol radiative effect

Table S3. Study areas selected for this study.

City Level	City Name
Province-level municipality	Beijing (BJ), Chongqing (CQ), Shanghai (SH), Tianjin (TJ)
Provincial capital city	Changchun (CC), Changsha (CS), Chengdu (CD), Fuzhou (FZ), Guangzhou (GZ), Guiyang (GY), Haerbin (HEB), Haikou (HK), Hangzhou (HZ), Hefei (HF), Huhehaote (HHHT), Jinan (JN), Kunming (KM), Lanzhou (LZ), Nanchang (NC), Nanjing (NJ), Nanning (NN), Shenyang (SY), Shijiazhuang (SJZ), Taiyuan (TY), Wuhan (WH) , Wulumuqi (WLMQ), Xi'an (XA), Xining (XN), Yinchuan (YC), Zhengzhou (ZZ)
Municipalities with independent planning status under the national social and economic development	Dalian (DL), Ningbo (NB), Qingdao (QD), Shenzhen (SZ), Xiamen (XM)